

FaceCat: Enhancing Face Recognition Security with a Unified Generative Model Framework

Jiawei Chen

chenjiawei@stu.ahu.edu.cn
Department of Computer Science & Technology, Anhui University

Xiao Yang*

yangxiao19@mails.tsinghua.edu.cn
Department of Computer Science & Technology, Tsinghua University

Yinpeng Dong

dongyinpeng@mails.tsinghua.edu.cn
Department of Computer Science & Technology, Tsinghua University

Hang Su

suhangss@tsinghua.edu.cn
Department of Computer Science & Technology, Tsinghua University

Jianteng Peng

pengjianteng@oppo.com
OPPO
Beijing, China

Zhaoxia Yin*

zxyin@cee.ecnu.edu.cn
East China Normal University
Shanghai, China

ABSTRACT

Face anti-spoofing (FAS) and adversarial detection (FAD) have been regarded as critical technologies to ensure the safety of face recognition systems. As a consequence of their limited practicality and generalization, some existing methods aim to devise a framework capable of concurrently detecting both threats to address the challenge. Nevertheless, these methods still encounter challenges of insufficient generalization and suboptimal robustness, potentially owing to the inherent drawback of discriminative models. Motivated by the rich structural and detailed features of face generative models, we propose **FaceCat** which utilizes the face generative model as a pre-trained model to improve the performance of FAS and FAD. Specifically, FaceCat elaborately designs a hierarchical fusion mechanism to capture rich face semantic features of the generative model. These features then serve as a robust foundation for a lightweight head, designed to execute FAS and FAD tasks simultaneously. As relying solely on single-modality data often leads to suboptimal performance, we further propose a novel text-guided multi-modal alignment strategy that utilizes text prompts to enrich feature representation, thereby enhancing performance. For fair evaluations, we build a comprehensive protocol with a wide range of 28 attack types to benchmark the performance. Extensive experiments validate the effectiveness of FaceCat generalizes significantly better and obtains excellent robustness against input transformations.

KEYWORDS

Face Recognition Security, Multi-modal Alignment, Diffusion Model

1 INTRODUCTION

Deep learning has propelled face recognition (FR) to the forefront of biometric applications, but its proliferation has sparked security concerns like presentation attacks [2, 38, 40] and adversarial attacks [15, 36, 61], which are crafted to deceive FR systems into granting unauthorized access or misidentifying individuals. In response to these challenges, specialized defense mechanisms have been developed, namely face anti-spoofing [21, 63, 64, 67] and face adversarial detection [11, 42]. Both of them are considered as two

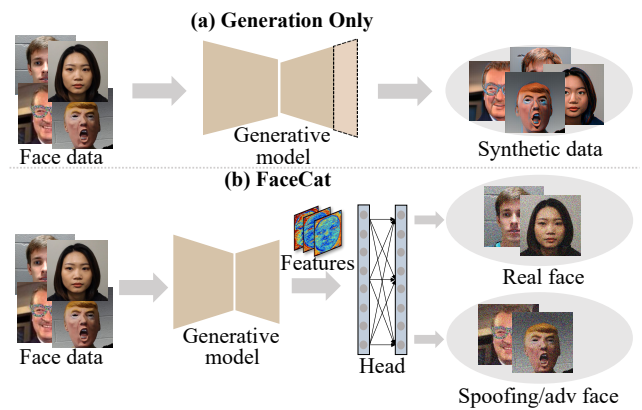


Figure 1: Comparison of our method and face generative models. (a) The face generation only models. (b) Our FaceCat exploits the abundant features inherent in face generative models to serve face anti-spoofing and adversarial detection simultaneously.

independent tasks by the existing methods. This suggests the necessity for deploying multiple models, thereby increasing the computational overhead. Moreover, recent research [6, 9, 62] indicates that these methods generally lack generalization ability (The FAS method cannot be directly applied to the detection of adversarial examples, and vice versa). In other words, these defenses cannot generalize well on unknown attack categories due to the overfitting to the manipulation types they are trained, limiting the practical applicability. Therefore, it is critical for FR systems to integrate these security tasks to improve their overall robustness against attacks.

Aiming to strengthen the overall robustness of the FR system, some studies [9, 62] have been concerned about the unification of these security vulnerabilities. These techniques address multiple attack categories simultaneously, aiming to create a more resilient system. However, due to the inherent drawback of discriminative models [57], such approaches tend to make models primarily focus on the structural features of images. This focus can lead to a narrow detection scope, potentially missing nuanced aspects like texture

*Corresponding author: Zhaoxia Yin and Xiao Yang

Table 1: Comparison of the proposed protocol with others.

Study	Presentation attack		Adversarial attack			Types
	2D	3D	perturbation	patch	3D-printed	
FaceGuard [8]	✓	✓	✓	✓	✓	6
SIM-Wv2 [40]	✓	✓	✓	✓	✓	14
WMCA [22]	✓	✓	✓	✓	✓	7
HQ-WMCA [28]	✓	✓	✓	✓	✓	10
HiFiMask [38]	✓	✓	✓	✓	✓	3
GrandFake [9]	✓	✓	✓	✓	✓	25
FaceCat (Ours)	✓	✓	✓	✓	✓	28

and coloration. Some research [39, 54] indicates that detailed features such as skin texture and coloration can markedly enhance the performance of the detection of attacks. Thus, the drawback leads to limited multi-level discriminative features, which could adversely affect their generalization ability and robustness [55].

On the contrary, face generative models (FGM) involve both the synthesis of face images and the nuanced manipulation of their attributes, which enable them to comprehend global structural and deep-level detailed features [47]. This enhancement greatly increases multi-level features, enabling it to hold foundational face knowledge that exceeds the scope of other models. Introducing FGM as a foundational model within the face security framework offers distinctive and rich knowledge priors. This serves as a potent addition to FAS and FAD tasks, contributing to enhanced performance of defense mechanisms, as illustrated in Figure 1.

Recent research [12] illustrates that diffusion models [29] produce high-quality images, surpassing previous state-of-the-art (SOTA) generative models [13, 35] in terms of image fidelity and detail. Given that enhanced image generation performance can translate to improved feature quality [59], we employ the face diffusion model (FDM) for this task. However, applying off-the-shelf FDM to face security tasks poses challenges due to substantial variations in facial semantic information across FDM blocks, complicating feature selection, as shown in Figure 3.

In this paper, we propose **FaceCat** which is the first framework to integrate FAS and FAD via a generative model. Specifically, we design a hierarchical fusion mechanism, which not only addresses the challenge of adapting FDM to face security tasks but also enhances FaceCat’s performance through the incorporation of multi-level features. We amalgamate five distinct hierarchical blocks and stack them through pooling operations to form a unified face feature, adept at seamless integration with downstream network architectures. Nonetheless, the efficacy of FAS and FAD is frequently compromised due to the inherent information limitations of relying solely on single-modal (RGB) data [21, 63]. Inspired by the fact that textual data can often provide richer information for computer vision [33], we propose a **text-guided (TG) multi-modal alignment strategy**, which utilizes text knowledge to enrich semantic content and thereby further enhance the model’s representation capability. In detail, we leverage the text encoder from CLIP [45] to generate text embeddings. These embeddings are then integrated with FDM’s image embeddings to compute a similarity score, which is regarded as the logit for optimization. Moreover, owing to the similarity of face features, a **triplet-based margin optimization** is adopted to make real samples more compact and push attack samples apart.

To evaluate the ability of different methods, we develop a comprehensive and fair protocol to perform FAS and FAD simultaneously. In particular, this protocol encompasses **28 diverse attack types**, involving multiple new practical attacks, such as 3D-printed attacks, as shown in Table 1. Based on this protocol, we compare FaceCat with several currently popular methods, including **five** FAS methods, **three** FAD methods, and **four** classification models. For the sake of fairness, all these methods have been fine-tuned on the proposed protocol. Moreover, three prevalent input transformations [18, 24] are adopted to verify the robustness of FaceCat. We also conduct the ablation study to further investigate the proposed components. Experimental results demonstrate that our method exhibits excellent performance and outstanding robustness. Our main contributions can be summarized as:

- We propose a novel perspective that considers the FDM as a pre-trained model, demonstrating that it contains a wealth of inherently robust face semantic features, which can serve as a strong initialization for integrating face anti-spoofing and adversarial detection.
- We propose a text-guided multi-modal alignment strategy with text embeddings which can enhance performance by leveraging multi-modal signals’ supervision.
- Extensive experiments demonstrate that the proposed method exhibits superior performance by utilizing FDM’s abundant prior knowledge, showcasing excellent robustness against multiple input transformations such as bit-depth reduction and JPEG compression.

2 RELATED WORK

In this section, we review related work on representation with generative models, face anti-spoofing, and adversarial detection. Furthermore, we delineate the distinctions between our FaceCat and existing approaches.

2.1 Representation with Generative Models

The concept of using generative learning for representation is long-established, due to its inherent intuitiveness. In the initial stages, pioneers attempt to exploit GANs [7, 13, 46] and VAEs [34, 35] for representation learning. [14, 58] demonstrate GANs can learn a competitive representation for images in latent space. Over the recent biennium, diffusion models [1, 30, 44] have garnered substantial achievements in the realm of generative learning, which are regarded as the SOTA generative models currently. Therefore, recent works attempt to utilize diffusion models for representation learning to serve downstream tasks, such as image editing [33], semantic segmentation [1], and image classification [44], etc. Despite achieving commendable performance, the majority of these studies lack investigation into integrating face security tasks and the robustness of diffusion models. In contrast, we demonstrate the rich feature semantics of diffusion models to execute FAS and FAD and confirm their robustness by subjecting them to tests with various common input transformations.

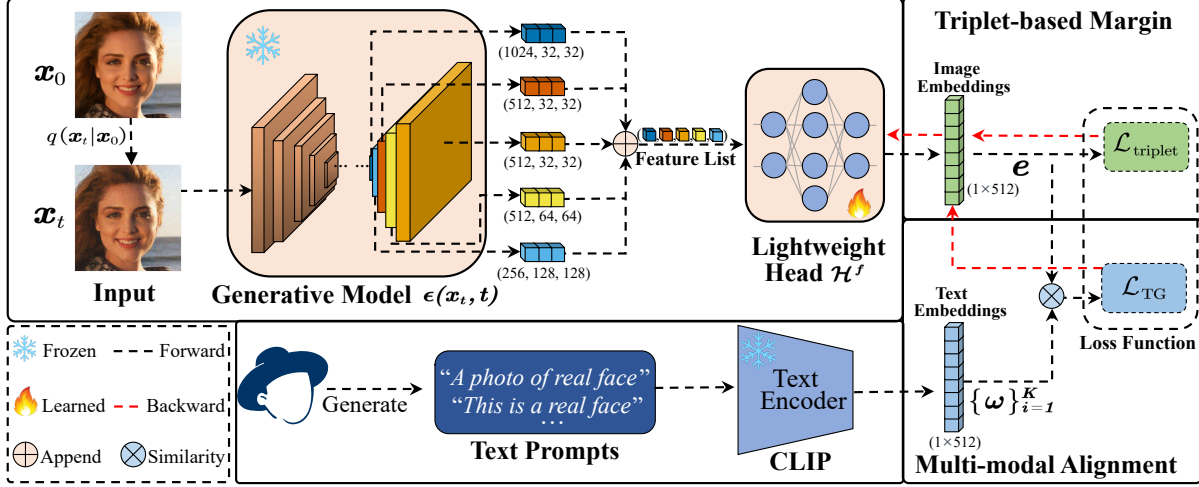


Figure 2: An overview of our proposed FaceCat framework. FaceCat includes a generative model $\epsilon(x_t, t)$ to encode the noisy image x_t into the face features, a lightweight head \mathcal{H}^f to extract image embeddings e from these face features, and a text encoder of CLIP to obtain text embeddings from text prompts. Through image embeddings and text embeddings $\{\omega\}_{i=1}^K$, the multi-modal alignment strategy calculates a text-image similarity score treated as the logit. The triplet-based margin is utilized to facilitate the learning of features.

2.2 Face Anti-Spoofing and Adversarial Detection

The appearance of presentation attacks and adversarial attacks are designed to trick face recognition systems into allowing unauthorized access or incorrectly identifying individuals. Thus, FAS [3, 6, 48, 67] and FAD [5, 11, 42, 43] have been developed to protect face recognition systems. In recent years, research in FAS has increasingly gravitated towards the exploration of 3D and multi-modal approaches [21, 28]. FAD exhibits a preference for the development of attack-agnostic, universally applicable defense methods [11, 56]. Moreover, some research [9, 62] attempts to unify several face security tasks into a framework, aiming to enhance both practicality and generalization. UniFAD [9] attempts to unify digital attacks and FAS through k-means clustering. JFSFD [62] establishes the first joint FAS and deepfake detection benchmark using both visual appearance and physiological rPPG cues. However, due to the inherent drawback of classification models, such methods primarily focus on the structural features of images. As a comparison, FaceCat has global structural and deep-level detailed features by virtue of its use of generative models. Furthermore, we introduce a comprehensive evaluation protocol for assessing the performance of FAS and FAD concurrently, as detailed in Table 1.

3 METHOD

We first formulate how to unify FAS and FAD in Section 3.1. Afterward, we propose a text-guided multi-modal alignment strategy for improving performance in Section 3.2. Moreover, a triplet-based margin optimization is utilized to auxilarily increase the distance between positive and negative samples in Section 3.3. In Section 3.4, we elucidate the technical details of the hierarchical fusion

mechanism and the lightweight head. An overview of our proposed method is provided in Figure 2.

3.1 Problem Formulation

For FAS and FAD tasks, we can define three input types: spoofing face x^{spoof} , adversarial face x^{adv} and real face x^{real} . As for a unified detector, it is only necessary to reject potential attack types without identifying whether x^{spoof} or x^{adv} . Thus, we define $x^{fake} \in \{x^{spoof}, x^{adv}\}$. The decision function can be defined as:

$$f_{\theta} : x \rightarrow \{0 (x^{fake}), 1 (x^{real})\},$$

which classifies whether a sample x is fake or real. $f_{\theta}(x) : \mathbb{R}^d \rightarrow \mathbb{R}$ is the unified detector parameterized by θ . Generally, the problem is formulated as a dichotomous classification as follows:

$$\mathcal{L}_c(x, y) = \mathbb{E}_{p(x)} [-y \log(f_{\theta}(x)) + (1 - y) \log(1 - f_{\theta}(x))],$$

where $y \in \{0, 1\}$, $x \in \{x^{fake}, x^{real}\}$, (1)

where y is the ground truth, $x \in \mathbb{R}^d$ is the input. In this paper, our method also considers unifying FAS and FAD as a dichotomous classification problem.

Traditional classification models may overly prioritize image structure at the expense of fine details, whereas FDM inherently contains rich global structural and deep-level detail features. Therefore, we aim to leverage it as a strong initialization for FAS and FAD. A brief overview of FDM reveals that its training process is structured in two stages: 1) The forward diffusion process gradually adds Gaussian noise to the data to obtain a sequence of noisy samples; 2) The backward generative process reverses the diffusion process to denoise images. The central objective is to predict the noise at time t , which is formulated as a simple mean squared error

loss:

$$\mathcal{L}_{\text{simple}} = \mathbb{E}_{\mathbf{x}_0, t, \epsilon} [\|\epsilon_{\psi}(\mathbf{x}_t, t) - \epsilon\|_2^2], \quad (2)$$

where ϵ_{ψ} is the diffusion models and \mathbf{x}_t is the noisy image at time t (noise level), i.e., \mathbf{x}_t is obtained by adding noise ϵ to \mathbf{x} .

In this paper, we focus on using the **Face** diffusion model as a **Catalyst (FaceCat)** for enhancing FAS and FAD. Formally, given a FDM ϵ_{ψ} , Note that we only obtain the features from the middle layer through ϵ_{ψ} , not the predicted noise, i.e., the input \mathbf{x}_t is processed through ϵ_{ψ} to obtain a universal face feature with dimension d' . To leverage this feature, a lightweight head $\mathcal{H} : \mathcal{R}^{d'} \rightarrow \mathcal{R}$ is adopt. Therefore, the objective function of FaceCat can be formulated as:

$$\min_{\kappa} \mathbb{E}_{p(\mathbf{x}_t)} [\mathcal{L}_c(\mathcal{H}_{\kappa}(\epsilon_{\psi}(\mathbf{x}_t, t)), y)], \quad (3)$$

where \mathcal{H} is parameterized by κ and $p(\mathbf{x}_t)$ is the probability distribution of \mathbf{x}_t . Note that Equation 3 is only adopted to optimize the lightweight head \mathcal{H}_{κ} . The rationale behind this is twofold: 1) The features of FDM are sufficiently general-purpose; 2) By not fine-tuning FDM, we significantly reduce the training time. By following the objective (3), given a face image \mathbf{x} , we can get the probability of whether it is a real face.

However, attributable to significant disparities in facial semantic information among distinct blocks of FDM, we usually obtain limited performance attributed to suboptimal choices of blocks. Based on this, we propose to adopt a hierarchical fusion mechanism to solve the challenge effectively, which not only tackles the task of adapting FDM for face security but also amplifies FaceCat’s capabilities by integrating multi-level features. Both structural and detailed face features are essential for face security tasks. Furthermore, as indicated by [19], larger blocks closer to the output tend to represent simpler patterns like edges and contours, while smaller blocks convey more abstract features. Therefore, we amalgamate five distinctive hierarchical blocks (more details in Section 3.4). Moreover, we consolidate them through pooling operations, leading to a unified facial feature that seamlessly integrates with the downstream network architecture.

Furthermore, adversarial and presentation attacks evolve rapidly, and the latter makes spoofing faces increasingly realistic. This indicates that it is inadequate for achieving optimal performance by relying solely on binary cross-entropy loss [21, 39]. Therefore, it is necessary to explore some new training strategies. We propose a text-guided multi-modal alignment strategy and use a triplet-based margin optimization to further improve our method, detailed in Section 3.2 and Section 3.3.

3.2 Text-guided Multi-modal Alignment

The performance of FAS and FAD often suffers due to the constraints associated with the exclusive use of single-modal (RGB) data. Drawing inspiration from the ability of textual data to impart more detailed information in computer vision tasks, we try to design a text-guided multi-modal alignment strategy so that text information can be used in face security models.

CLIP is trained on image-text pairs to align image features with text-derived classification weights. Given a batch of image-text pairs, CLIP can predict the image’s class by computing a text-image cosine similarity. Formally, given an image \mathbf{x} , we can compute the

Table 2: The text prompts of the real and fake classes.

	Text Prompts
Real Prompts	A photo of a real face. This is a real face. This is not a fake face. An example of a real face. A photo of the bonafide face. An example of a bonafide face.
Fake Prompts	A photo of a fake face. This is a fake face. This is not a real face. An example of a fake face. A photo of the attack face. An example of attack face.

prediction probability as follows:

$$p(\hat{y}|\mathbf{x}) = \frac{\exp(\cos(\omega_i, \mathbf{e})/\tau)}{\sum_{j=1}^K \exp(\cos(\omega_j, \mathbf{e})/\tau)}, \quad (4)$$

where τ is a temperature parameter and \hat{y} is the predicted class label. \mathbf{e} is the image embedding of \mathbf{x} extracted by the image encoder, and $\{\omega\}_{i=1}^K$ represent the weight vectors from the text encoder. K and $\cos(\cdot, \cdot)$ denote the number of classes and cosine similarity, respectively.

Specifically, we craft some text prompts for this task along the lines of “a photo of a [class]”. The “[class]” is “[real face]” or “[fake face]”, all text prompts are presented in Table 2. This can be formalized as $\mathbf{t} = [V]_1[V]_2 \dots [V]_M[\text{real/fake face}]$, where each $[V]_m (m \in \{1, \dots, M\})$ is a vector with the same dimension as word embeddings (i.e., 512 for CLIP), and M is a hyperparameter specifying the number of context tokens. Given the CLIP’s text encoder $g(\cdot)$, we can obtain $\omega = g(\mathbf{t})$.

As for \mathbf{e} , we can acquire through the lightweight head \mathcal{H} . Assume that the feature layer of \mathcal{H} is $\mathcal{H}^f : \mathcal{R}^{d'} \rightarrow \mathcal{R}^{d''}$, where $d'' = 512$ which matches the dimension of word embeddings. Hence, Equation 4 can be re-expressed as:

$$p(\hat{y}|\mathbf{x}_t) = \frac{\exp(\cos(g(\mathbf{t}), \mathcal{H}^f(\epsilon_{\psi}(\mathbf{x}_t)))/\tau)}{\sum_{j=1}^K \exp(\cos(g(\mathbf{t}), \mathcal{H}^f(\epsilon_{\psi}(\mathbf{x}_t)))/\tau)}, \quad (5)$$

where $K = 2$ and \mathbf{x}_t is the noisy image. Additionally, we employ the more flexible focal loss [37] as the optimization function instead of binary cross-entropy loss. Formally, given that p denotes the probability in $p(\hat{y}|\mathbf{x}_t)$ that the identified image is a real face, we adopt the notation p_c to represent the probability of the target class:

$$p_c = \begin{cases} p & \text{if } y = 1, \\ 1 - p & \text{otherwise.} \end{cases} \quad (6)$$

Referring to the standard α -balanced focal loss [37], the text-guided multi-modal alignment can be formulated as follows:

$$\text{TG}(p_c, y) = -\alpha_c (1 - p_c)^y \log(p_c), \quad (7)$$

the parameter α_c is introduced to balance the data distribution, and its formal definition mirrors that of Equation 6, with p replaced by α . Since negative samples are approximately twice as many as

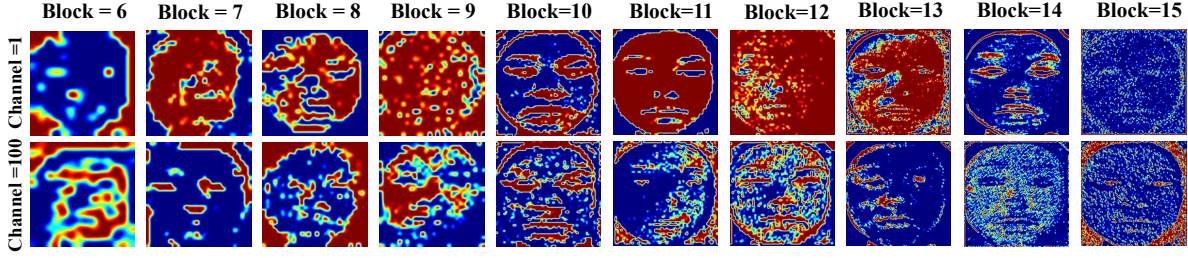


Figure 3: Multi-block feature representations are derived from the face diffusion model across different channels.

positive samples, α is set to 0.75. To encourage \mathcal{H}^f to focus on hard samples during training, we set the focusing parameter γ to 2.0.

3.3 Triplet-based Margin Optimization

Face data from different classes exhibits similar features, which is different from general classification tasks. This characteristic makes it difficult to distinguish between positive and negative sample features. Therefore, we adopt a triplet loss [27] to supervise features, which is commonly utilized in deep metric learning, and has proven its effectiveness in optimizing the relative distances between samples in the embedded space. The mathematical form is expressed as follows:

$$\mathcal{L}_{\text{triplet}}(\mathbf{x}^a, \mathbf{x}^p, \mathbf{x}^n) = \max\left(0, \left\| \mathcal{H}^f(\epsilon_{\psi}(\mathbf{x}^a)) - \mathcal{H}^f(\epsilon_{\psi}(\mathbf{x}^p)) \right\|_2^2 - \left\| \mathcal{H}^f(\epsilon_{\psi}(\mathbf{x}^a)) - \mathcal{H}^f(\epsilon_{\psi}(\mathbf{x}^n)) \right\|_2^2 + m\right),$$

where \mathbf{x}^p and \mathbf{x}^n are the positive sample (\mathbf{x}^{real}) and negative samples (\mathbf{x}^{fake}) respectively. \mathbf{x}^a is an anchor sample, which is the same class as \mathbf{x}^{real} . $\|\cdot\|_2^2$ represents the squared Euclidean distance. The margin m is a hyperparameter ensuring a safe gap between positive and negative pairs, preventing trivial solutions. Therefore, Equation 3 can be rewritten as:

$$\min_{\kappa'} \mathbb{E}_{p(\mathbf{x}_t)} \left[\text{TG}(p_c, y) + \lambda \cdot \mathcal{L}_{\text{triplet}}(\mathbf{x}_t^a, \mathbf{x}_t^{real}, \mathbf{x}_t^{fake}) \right], \quad (8)$$

where κ' denotes the parameters of \mathcal{H}^f . λ is the balancing factor. $\mathbf{x}_t^a, \mathbf{x}_t^{real}$ and \mathbf{x}_t^{fake} represent the forms of $\mathbf{x}^a, \mathbf{x}^{real}$ and \mathbf{x}^{fake} with the addition of noise. Note that we also do not optimize the parameters of $g(\cdot)$. Following Equation 8, we can acquire a classifier that performs FAS and FAD simultaneously.

3.4 Hierarchical Fusion Mechanism and Lightweight Head

As illustrated in Figure 3, different blocks of the diffusion model capture distinct facial features, with some layers representing detailed features and others abstract features. For facial security tasks, both types of features are beneficial to model performance. Thus, we propose leveraging a hierarchical fusion mechanism to integrate these diverse features:

$$f_{total} = \sum_{i=1}^n \mathcal{F}_i(f_i), \quad (9)$$

Table 3: The performance of FaceCat with different blocks.

	Performance		
	ACER	EER	TDR@0.2%FDR
B = 5, 6	2.62	2.59	92.81
B = 7, 8	2.67	2.74	92.89
B = 5, 12	2.82	2.79	92.58
B = 5, 6, 7, 12	2.56	2.40	93.07
B = 5, 6, 7, 8	2.51	2.45	93.19
B = 5, 6, 7, 8, 12	2.29	2.35	93.56

where f_i denotes the input features to the i^{th} block, and $\mathcal{F}_i(f_i)$ represents the output features after processing by the i^{th} block. f_{total} is the features after fusion. For the lightweight head, aiming for minimal weight while ensuring performance, we utilize the first four layers of ResNet-18, complemented by an additional two downsampling layers.

Although some related works [39] have also introduced the concept of multi-level features, their application has largely been empirical within traditional classification models. Given the unique architecture of diffusion models, which differs significantly from conventional classification models, previous experiences cannot be directly applied. Consequently, our investigation into the fusion of different blocks is detailed in Table 3. Observations indicate that optimal performance is achieved when blocks 5, 6, 7, 8, 12 are selected. Consequently, this configuration has been adopted for subsequent experiments.

4 EXPERIMENTS

This section is organized to meticulously outline the evaluation process of our proposed method. Initially, we embark on a comprehensive series of experiments designed to rigorously assess the efficacy and robustness of our approach under various conditions. Subsequently, to shed light on the significance of each component within our system, we conduct detailed ablation studies, thereby highlighting their importance in achieving the overall performance of our method. Furthermore, to underscore the practicality and real-world applicability of our approach, we present evidence of its effectiveness in defending against sophisticated attacks, specifically 3D-printed adversarial examples.

Table 4: The different performances comparison (%) between the proposed FaceCat and baseline methods under the protocol.

	Method	Performance				
		APCER	BPCER	ACER	EER	TDR @ 0.2% FDR
Face anti-spoofing	CDCN [64]	3.38	2.86	3.12	3.16	88.42
	CMFL [21]	3.43	3.19	3.31	3.32	85.94
	DeepPixBis [20]	1.89	3.63	2.76	3.12	85.48
	Depthnet [39]	2.64	5.53	4.09	4.23	88.81
	FRT-PAD [67]	2.80	3.04	2.52	2.93	89.20
Face adversarial detection	EST [43]	5.29	2.01	3.65	3.89	88.31
	FDS [5]	4.89	3.22	4.06	3.54	87.43
	DFRAA [42]	3.52	3.12	3.32	3.26	88.19
Classification models	Resnet50 [26]	3.84	2.77	3.31	3.36	86.41
	Inceptionv3 [49]	2.91	3.69	3.30	3.35	87.54
	Efficientnetb0 [50]	3.80	3.23	3.52	3.53	86.44
	ViT-b/16 [17]	3.31	3.02	3.17	3.18	87.56
Proposed FaceCat	w/o TG	1.96	2.70	2.33	2.35	92.74
	with TG	1.80	2.79	2.29	2.35	93.56

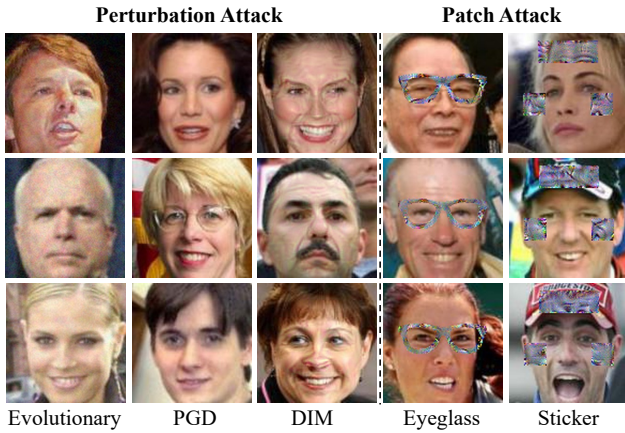


Figure 4: The adversarial examples with different attacks.

4.1 Experimental Settings

Datasets and protocols. To evaluate FaceCat’s capacity for concurrent FAS and FAD, we first craft 14 adversarial examples from the LFW [31] dataset targeting the state-of-the-art (SOTA) face recognition model, ArcFace [10], as shown in Figure 4. We employ various techniques including 1) adversarial perturbation: FGSM(w) [23], PGD(w) [41], DIM(w) [60] and Evolutionary(b) [16]; 2) adversarial patch [51]: Eyeglass(w), Sticker(w), Facemask(w). The ‘w’ and ‘b’ represent white and black-box attacks respectively. Each attack type contains dodging and impersonation attacks. The attack success rate (ASR) and more adversarial examples are shown in Appendix A. Moreover, SiW-Mv2 is adopted as a complement to evaluate FAS. We partition the adversarial examples based on Protocol 1 of SiW-Mv2 and subsequently incorporate them into SiW-Mv2. Therefore, we obtain a comprehensive protocol to evaluate FAS and FAD simultaneously.

Evaluation metrics. We evaluate with the following metrics: Attack Presentation Classification Error Rate (APCER), Bona Fide Presentation Classification Error Rate (BPCER), and the average of APCER and BPCER, Average Classification Error Rate (ACER) for a fair comparison. Equal Error Rate (EER), Area Under Curve (AUC), and True Detection Rate (TDR) at a False Detection Rate (FDR) 0.2% (TDR @ 0.2% FDR¹). In addition, a visualization [52] is also reported to evaluate the performance further.

Training details. The face generative model [1] employed in our study has been specifically trained on the FFHQ [32] dataset to enable sophisticated generation of face images. The specific training details are fully aligned with the steps outlined in [1]. The input images are cropped using MTCNN [65] and resized to 256×256. We utilize the Stochastic Gradient Descent (SGD) optimizer for training our FaceCat. The training phase and learning rate are initialized to 30 epochs and 1e-2 respectively, and we incorporate a momentum of 0.9 to accelerate the optimizer in the relevant direction and dampen oscillations. Additionally, we employ weight decay with a coefficient of 5e-4 to provide a regularization effect, helping prevent overfitting. To dynamically adjust the learning rate during training, we use a Cosine Annealing learning rate scheduler that spans across the total number of epochs. The balancing factor λ in Equation 8 is set to 0.1.

4.2 Experiment in the Proposed Protocol

Effectiveness of the proposed method. To verify the efficacy of the proposed approach, we compare FaceCat with three baselines: 1) FAS: CDCN [64], CMFL [21], DeepPixBis [20], Depthnet [39], FRT-PAD [67]; 2) FAD: EST [43], FDS [5], DFRAA [42]; 3) classification models: Resnet50 [26], Inceptionv3 [49], Efficientnetb0 [50], ViT-b/16 [17]. These methods are either commonly used or represent the SOTA techniques. To fairly compare the proposed method, all these methods have been fine-tuned according to the proposed protocol. Table 4 shows the performance metrics for each method.

¹<https://www.iarpa.gov/index.php/research-programs/odim>

Inspection of the table allows us to deduce the subsequent conclusions:

(1) FaceCat effectively improves the overall security of the face recognition systems. When conducting FAS and FAD simultaneously, the TDR @ 0.2% FDR and ACER exhibit a relative increase of at least 4.36% and 9.13% over the baselines, respectively. We attribute this advancement to the unique and abundant knowledge priors inherent in FDM, which significantly enhance multi-level features, thereby enabling the proposed method to acquire more sophisticated face representations. As shown in Figure 3, we visually elucidate the variations in feature representations across distinct blocks, thereby offering supplementary evidence to substantiate the consistency of the hierarchical fusion mechanism.

(2) The proposed method with the text-guided multi-modal alignment strategy generally outperforms the variant without it across various metrics. This demonstrates the strategy can effectively improve the performance of the proposed method. We think it benefits from low-cost and effective text embedding, which facilitates face features learning under the nuanced supervision of multi-modal cues.

(3) It is noteworthy that FRT-PAD [67] demonstrates commendable performance at the baselines, owing in part to its utilization of face related tasks’ models as a backbone. This leads to two infeasible propositions: Firstly, using prior knowledge of face related tasks can augment the effectiveness of FAS and FAD, i.e., this could represent a promising avenue for enhancing the security of face recognition systems. Secondly, FDM outperforms other approaches that leverage face-related tasks as priors, attributable to its richness in global structural features and deep-level detailed features.

Evaluation on input transformation. To evaluate the robustness of FaceCat, common input transformations (such as bit-depth reduction, Gaussian blur, and JPEG compression) are employed to reduce the image quality. Note that these input transformations are not included in the data augmentation. We choose to benchmark our results with a widely recognized method, CDCN [64]. Here, we employ Area Under Curve (AUC) as a measure of performance, which is a comprehensive metric. As shown in Figure 5, when image quality degrades, the performance of the baseline in addressing diverse types of attacks diminishes, with its response to JPEG compression being the most notably affected. This indicates that although the baseline can demonstrate decent performance under the proposed protocol, its robustness significantly decreases with the degradation of image quality. In contrast, FaceCat continues to maintain stable performance even in the face of degraded image quality, reaching up to 55.3% better than the baseline under JPEG compression. This can be attributed to the superior feature robustness of FaceCat, i.e., even with the loss of certain image information, the proposed method is still sufficient to achieve robust metrics in detecting such attack threats.

4.3 Ablation Study

Advantages of FDM architecture. We conduct ablation experiments to verify the effectiveness of FDM architecture, as shown in the first three rows of Table 5. Both MAE [25] and SwAV [4] represent state-of-the-art self-supervised learning methodologies

Table 5: The ablation study results of FaceCat in the protocol.

Method	Performance		
	ACER	EER	TDR@0.2%FDR
MAE [25]	2.33	2.36	92.77
SwAV [4]	2.36	2.23	91.57
FR-ArcFace [10]	2.75	2.41	91.14
w/o clip ($\alpha=0.25$)	2.74	2.76	88.66
w/o clip ($\alpha=0.5$)	2.89	3.02	91.58
w/o clip ($\alpha=0.75$)	2.33	2.36	92.74
FaceCat	2.29	2.35	93.56

that have undergone pre-training on the FFHQ dataset prior to fine-tuning on our proposed protocol, ensuring consistency in model initialization. The FR-ArcFace [10] is the face recognition model ArcFace, which utilizes a ResNet18 [26] backbone and is pre-trained for face recognition tasks. From the table, two key conclusions can be drawn: Firstly, even the employment of pre-trained face models can enhance the model’s capabilities in conducting FAS and FAD; however, FDM, with its dual focus on global structural information and intricate detail features, demonstrates superior performance over these pre-trained face models. Secondly, utilizing face recognition models as pre-trained systems yields inferior results compared to models pre-trained via self-supervised methods. This is attributed to the tendency of classification models to overemphasize structural features, resulting in a partial loss of feature information.

Feature visualization. The feature distribution in the test set on the proposed protocol is visualized in Figure 6 via t-SNE [52], which consists of 6 types (live, PGD, makeup, silicone mask, facemask, transparent mask). Through the figure, it is evident from (b) that, in the absence of TG, facemask and PGD are not distinctly separable. Moreover, the live sample distribution from (a) is compact and the clusters exhibit improved separation for the proposed method trained with TG. These results illustrate the effectiveness of the text-guided strategy in FAS and FAD tasks. The main reason is that TG can leverage text embeddings to enhance the aggregation and distinction of image features.

Value of hyper-parameter α . In Table 5, we exploit the influence of different hyper-parameter α of TG on the experimental results. $\alpha = 0.75$ performs better than other settings. Furthermore, the best performance can be achieved when adopting the text-guided multi-modal alignment strategy and $\alpha = 0.75$. In joint defense scenarios, the quantity and diversity of real face samples are typically inferior to those of spoofing faces. This leads to an imbalanced focus of models on fake face samples. In the absence of appropriate constraints, the utilization of binary cross-entropy loss tends to excessively prioritize fake face data while neglecting valuable information from genuine face features. Therefore, adjusting hyper-parameter α to mitigate sample imbalance significantly improves the model’s overall performance.

How to determine the timestep t ? Although we have highlighted the remarkable representation power of FDM, the optimal utilization of this potential remains to warrant further exploration. Moreover, the experimental results (in Table 6) indicate that our FaceCat shows distinct performance due to different timesteps t .

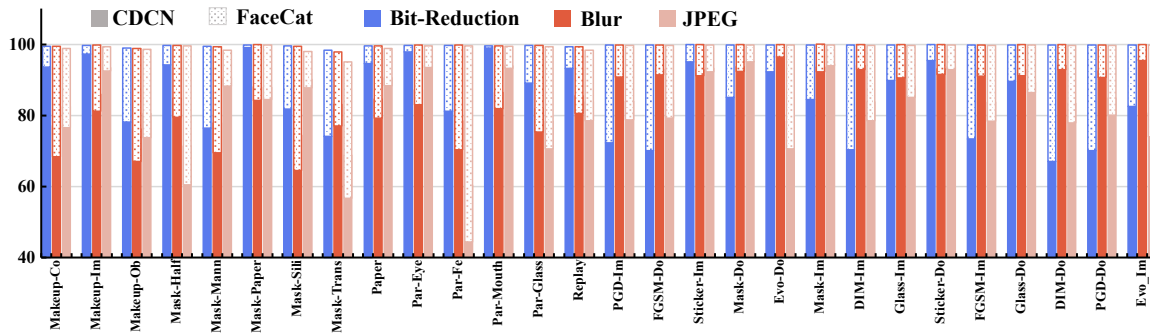


Figure 5: The area under curve (%) between FaceCat and the baseline against common input transformations.

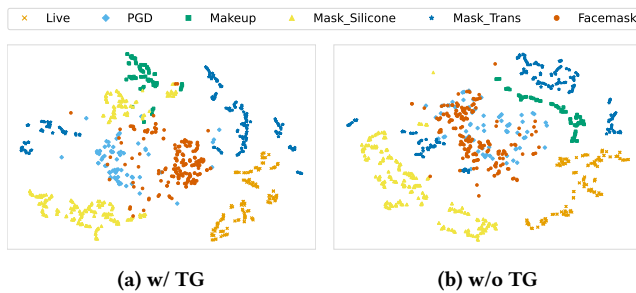


Figure 6: Feature distribution visualization of the test set on the proposed protocol using t-SNE [52]. (a) Features with TG. (b) Features without TG.

Table 6: The performance of FaceCat with different timesteps.

	Performance		
	ACER	EER	TDR@0.2%FDR
t = 10	2.91	2.87	92.11
t = 50	2.29	2.35	93.56
t = 100	2.73	2.57	92.67

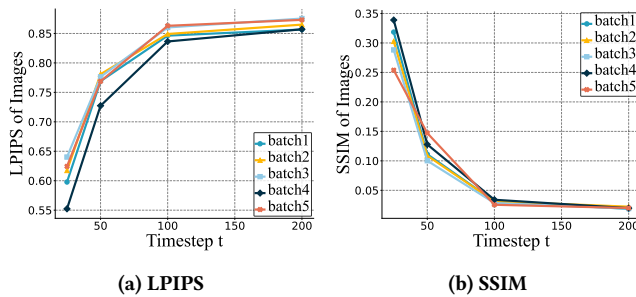


Figure 7: The quality of face images at various timesteps t .

Therefore, we further explore the impact of timestep. The timestep t is an essential parameter for FDM in representation learning. Our experiment indicates that when t is set too small, the representation

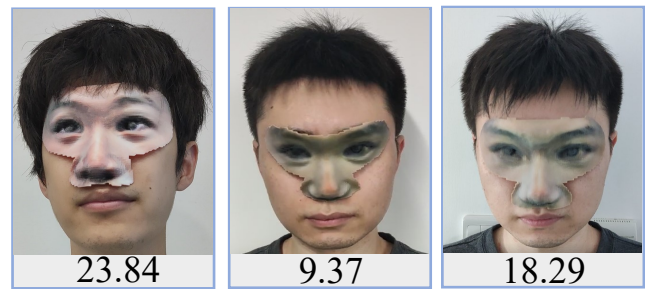


Figure 8: The experimental results of 3D-printed attacks.

capability is compromised. This suboptimal performance can potentially be attributed to the misalignment with the training process of the FDM. However, when t is set too large, it risks undermining the face semantic information. We plot the curves of LPIPS [66] and SSIM [53] during the step increasing, as illustrated in Figure 7, both indicators indicate that the quality of images is poor when the step is increased to 100. Hence, we set $t = 50$ as a balanced compromise.

4.4 Experiment in the Physical World

To evaluate the efficacy of our method in real-world scenarios, we adopt the technique described in [61] to generate 5000 3D-printed adversarial examples, which are currently proven to be one of the most challenging adversarial examples [61], as visualized in Figure 8. Note that we deliberately exclude this type from the training set to evaluate the generalizability of the proposed method rigorously. As shown in Table 7, our approach demonstrates consistent reliability and effectiveness when confronted with the challenge of identifying threats posed by adversarial attacks that utilize 3D printing technology. This phenomenon demonstrates that the proposed method can not only deal with known attacks well, but also generalize to unknown and more threatening attacks. This benefits from the unified face features derived from the FDM and the efficacy of our training strategy, which lead to a compact representation of real face features and a broader generalization of fake face characteristics.

Table 7: The performance of FaceCat in the physical world.

	Performance		
	ACER	EER	TDR@0.2%FDR
FaceCat	2.98	4.40	94.50

5 CONCLUSION

In this paper, we proposed a novel framework called FaceCat, which treats the FDM as a pre-trained model for integrating face anti-spoofing and adversarial detection. Besides, we introduced a text-guided multi-modal alignment and hierarchical fusion mechanism to enhance semantic information and optimize the utilization of FDM’s features, respectively. We also conducted extensive experiments to evaluate the effectiveness of FaceCat for face security tasks. Moreover, we further validated its robustness against common input transformations and the capability of generalization in real-world scenarios.

REFERENCES

- [1] Dmitry Baranchuk, Ivan Rubachev, Andrey Voynov, Valentin Khrukov, and Artem Babenko. 2021. Label-efficient semantic segmentation with diffusion models. *arXiv preprint arXiv:2112.03126* (2021).
- [2] Zinelabinde Boulkenafet, Jukka Komulainen, Lei Li, Xiaoyi Feng, and Abdenour Hadid. 2017. OULU-NPU: A mobile face presentation attack database with real-world variations. In *2017 12th IEEE international conference on automatic face & gesture recognition (FG 2017)*. IEEE, 612–618.
- [3] Rizhao Cai, Yawen Cui, Zhi Li, Zitong Yu, Haoliang Li, Yongjian Hu, and Alex Kot. 2023. Rehearsal-Free Domain Continual Face Anti-Spoofing: Generalize More and Forget Less. *arXiv preprint arXiv:2303.09914* (2023).
- [4] Mathilde Caron, Ishan Misra, Julien Mairal, Priya Goyal, Piotr Bojanowski, and Armand Joulin. 2020. Unsupervised learning of visual features by contrasting cluster assignments. *Advances in neural information processing systems* 33 (2020), 9912–9924.
- [5] Fabio Carrara, Rudy Becarelli, Roberto Caldelli, Fabrizio Falchi, and Giuseppe Amato. 2018. Adversarial examples detection in features distance spaces. In *Proceedings of the European conference on computer vision (ECCV) workshops*. 0–0.
- [6] Jiawei Chen, Xiao Yang, Heng Yin, Mingzhi Ma, Bihui Chen, Jianteng Peng, Yandong Guo, Zhaoxia Yin, and Hang Su. 2023. AdvFAS: A robust face anti-spoofing framework against adversarial examples. *Computer Vision and Image Understanding* 235 (2023), 103779.
- [7] Antonia Creswell, Tom White, Vincent Dumoulin, Kai Arulkumaran, Biswa Sengupta, and Anil A Bharath. 2018. Generative adversarial networks: An overview. *IEEE signal processing magazine* 35, 1 (2018), 53–65.
- [8] Debayan Deb, Xiaoming Liu, and Anil K Jain. 2023. Faceguard: A self-supervised defense against adversarial face images. In *2023 IEEE 17th International Conference on Automatic Face and Gesture Recognition (FG)*. IEEE, 1–8.
- [9] Debayan Deb, Xiaoming Liu, and Anil K Jain. 2023. Unified detection of digital and physical face attacks. In *2023 IEEE 17th International Conference on Automatic Face and Gesture Recognition (FG)*. IEEE, 1–8.
- [10] Jiankang Deng, Jia Guo, Niannan Xue, and Stefanos Zafeiriou. 2019. Arcface: Additive angular margin loss for deep face recognition. In *Proceedings of the IEEE/CVF conference on computer vision and pattern recognition*. 4690–4699.
- [11] Zhijie Deng, Xiao Yang, Shizhen Xu, Hang Su, and Jun Zhu. 2021. Libre: A practical bayesian approach to adversarial detection. In *Proceedings of the IEEE/CVF conference on computer vision and pattern recognition*. 972–982.
- [12] Prafulla Dhariwal and Alexander Nichol. 2021. Diffusion models beat gans on image synthesis. *Advances in neural information processing systems* 34 (2021), 8780–8794.
- [13] Jeff Donahue, Philipp Krähenbühl, and Trevor Darrell. 2016. Adversarial feature learning. *arXiv preprint arXiv:1605.09782* (2016).
- [14] Jeff Donahue and Karen Simonyan. 2019. Large scale adversarial representation learning. *Advances in neural information processing systems* 32 (2019).
- [15] Yinpeng Dong, Hang Su, Baoyuan Wu, Zhifeng Li, Wei Liu, Tong Zhang, and Jun Zhu. 2019. Efficient decision-based black-box adversarial attacks on face recognition. In *Proceedings of the IEEE/CVF Conference on Computer Vision and Pattern Recognition*. 7714–7722.
- [16] Yinpeng Dong, Hang Su, Baoyuan Wu, Zhifeng Li, Wei Liu, Tong Zhang, and Jun Zhu. 2019. Efficient decision-based black-box adversarial attacks on face recognition. In *Proceedings of the IEEE/CVF Conference on Computer Vision and Pattern Recognition*. 7714–7722.
- [17] Alexey Dosovitskiy, Lucas Beyer, Alexander Kolesnikov, Dirk Weissenborn, Xi-aohua Zhai, Thomas Unterthiner, Mostafa Dehghani, Matthias Minderer, Georg Heigold, Sylvain Gelly, et al. 2020. An image is worth 16x16 words: Transformers for image recognition at scale. *arXiv preprint arXiv:2010.11929* (2020).
- [18] Gintare Karolina Dziugaite, Zoubin Ghahramani, and Daniel M Roy. 2016. A study of the effect of jpeg compression on adversarial images. *arXiv preprint arXiv:1608.00853* (2016).
- [19] Wele Gedara Chaminda Bandara, Nithin Gopalakrishnan Nair, and Vishal M Patel. 2022. Remote Sensing Change Detection (Segmentation) using Denoising Diffusion Probabilistic Models. *arXiv e-prints* (2022), arXiv:2206.
- [20] Anjith George and Sébastien Marcel. 2019. Deep pixel-wise binary supervision for face presentation attack detection. In *2019 International Conference on Biometrics (ICB)*. IEEE, 1–8.
- [21] Anjith George and Sébastien Marcel. 2021. Cross modal focal loss for rgb-d face anti-spoofing. In *Proceedings of the IEEE/CVF conference on computer vision and pattern recognition*. 7882–7891.
- [22] Anjith George, Zohreh Mostaani, David Geissenbuhler, Olegs Nikisins, André Anjos, and Sébastien Marcel. 2019. Biometric face presentation attack detection with multi-channel convolutional neural network. *IEEE transactions on information forensics and security* 15 (2019), 42–55.
- [23] Ian J Goodfellow, Jonathon Shlens, and Christian Szegedy. 2014. Explaining and harnessing adversarial examples. *arXiv preprint arXiv:1412.6572* (2014).
- [24] Shuangchi Gu, Ping Yi, Ting Zhu, Yao Yao, and Wei Wang. 2019. Detecting adversarial examples in deep neural networks using normalizing filters. *UMBC Student Collection* (2019).
- [25] Kaiming He, Xinlei Chen, Saining Xie, Yanghao Li, Piotr Dollár, and Ross Girshick. 2022. Masked autoencoders are scalable vision learners. In *Proceedings of the IEEE/CVF conference on computer vision and pattern recognition*. 16000–16009.
- [26] Kaiming He, Xiangyu Zhang, Shaoqing Ren, and Jian Sun. 2016. Deep residual learning for image recognition. In *Proceedings of the IEEE conference on computer vision and pattern recognition*. 770–778.
- [27] Alexander Hermans, Lucas Beyer, and Bastian Leibe. 2017. In defense of the triplet loss for person re-identification. *arXiv preprint arXiv:1703.07737* (2017).
- [28] Guillaume Heusch, Anjith George, David Geissbühler, Zohreh Mostaani, and Sébastien Marcel. 2020. Deep models and shortwave infrared information to detect face presentation attacks. *IEEE Transactions on Biometrics, Behavior, and Identity Science* 2, 4 (2020), 399–409.
- [29] Jonathan Ho, Ajay Jain, and Pieter Abbeel. 2020. Denoising diffusion probabilistic models. *Advances in neural information processing systems* 33 (2020), 6840–6851.
- [30] Jonathan Ho, Ajay Jain, and Pieter Abbeel. 2020. Denoising diffusion probabilistic models. *Advances in neural information processing systems* 33 (2020), 6840–6851.
- [31] Gary B Huang, Marwan Mattar, Tamara Berg, and Eric Learned-Miller. 2008. Labeled faces in the wild: A database for studying face recognition in unconstrained environments. In *Workshop on faces in 'Real-Life' Images: detection, alignment, and recognition*.
- [32] Tero Karras, Samuli Laine, and Timo Aila. 2019. A style-based generator architecture for generative adversarial networks. In *Proceedings of the IEEE/CVF conference on computer vision and pattern recognition*. 4401–4410.
- [33] Gwanghyun Kim, Taesung Kwon, and Jong Chul Ye. 2022. Diffusionclip: Text-guided diffusion models for robust image manipulation. In *Proceedings of the IEEE/CVF Conference on Computer Vision and Pattern Recognition*. 2426–2435.
- [34] Durk P Kingma, Shakir Mohamed, Danilo Jimenez Rezende, and Max Welling. 2014. Semi-supervised learning with deep generative models. *Advances in neural information processing systems* 27 (2014).
- [35] Diederik P Kingma and Max Welling. 2013. Auto-encoding variational bayes. *arXiv preprint arXiv:1312.6114* (2013).
- [36] Stepan Komkov and Aleksandr Petiushko. 2021. Advhat: Real-world adversarial attack on arcface face id system. In *2020 25th International Conference on Pattern Recognition (ICPR)*. IEEE, 819–826.
- [37] Tsung-Yi Lin, Priya Goyal, Ross Girshick, Kaiming He, and Piotr Dollár. 2017. Focal loss for dense object detection. In *Proceedings of the IEEE international conference on computer vision*. 2980–2988.
- [38] Ajian Liu, Chenxu Zhao, Zitong Yu, Anyang Su, Xing Liu, Zijian Kong, Jun Wan, Sergio Escalera, Hugo Jair Escalante, Zhen Lei, et al. 2021. 3d high-fidelity mask face presentation attack detection challenge. In *Proceedings of the IEEE/CVF International Conference on Computer Vision*. 814–823.
- [39] Yaojie Liu, Amin Jourabloo, and Xiaoming Liu. 2018. Learning deep models for face anti-spoofing: Binary or auxiliary supervision. In *Proceedings of the IEEE conference on computer vision and pattern recognition*. 389–398.
- [40] Yaojie Liu, Joel Stehouwer, Amin Jourabloo, and Xiaoming Liu. 2019. Deep tree learning for zero-shot face anti-spoofing. In *Proceedings of the IEEE/CVF Conference on Computer Vision and Pattern Recognition*. 4680–4689.
- [41] Aleksander Madry, Aleksandar Makelov, Ludwig Schmidt, Dimitris Tsipras, and Adrian Vladu. 2017. Towards deep learning models resistant to adversarial attacks. *arXiv preprint arXiv:1706.06083* (2017).
- [42] Fabio Valerio Massoli, Fabio Carrara, Giuseppe Amato, and Fabrizio Falchi. 2021. Detection of face recognition adversarial attacks. *Computer Vision and Image Understanding* 202 (2021), 103103.
- [43] Abhishek Moitra, Youngeun Kim, and Priyadarshini Panda. 2022. Adversarial Detection without Model Information. *arXiv preprint arXiv:2202.04271* (2022).
- [44] Soumik Mukhopadhyay, Matthew Gwilliam, Vatsal Agarwal, Namitha Padmanabhan, Archana Swaminathan, Srinidhi Hegde, Tianyi Zhou, and Abhinav Shrivastava. 2023. Diffusion Models Beat GANs on Image Classification. *arXiv preprint arXiv:2307.08702* (2023).
- [45] Alec Radford, Jong Wook Kim, Chris Hallacy, Aditya Ramesh, Gabriel Goh, Sandhini Agarwal, Girish Sastry, Amanda Askell, Pamela Mishkin, Jack Clark, et al. 2021. Learning transferable visual models from natural language supervision. In *International conference on machine learning*. PMLR, 8748–8763.
- [46] Alec Radford, Luke Metz, and Soumith Chintala. 2015. Unsupervised representation learning with deep convolutional generative adversarial networks. *arXiv preprint arXiv:1511.06434* (2015).
- [47] Aditya Ramesh, Mikhail Pavlov, Gabriel Goh, Scott Gray, Chelsea Voss, Alec Radford, Mark Chen, and Ilya Sutskever. 2021. Zero-shot text-to-image generation. In *International Conference on Machine Learning*. PMLR, 8821–8831.
- [48] Koushik Srivatsan, Muzammal Naseer, and Karthik Nandakumar. 2023. FLIP: Cross-domain Face Anti-spoofing with Language Guidance. In *Proceedings of the IEEE/CVF International Conference on Computer Vision*. 19685–19696.
- [49] Christian Szegedy, Sergey Ioffe, Vincent Vanhoucke, and Alexander Alemi. 2017. Inception-v4, inception-resnet and the impact of residual connections on learning. In *Proceedings of the AAAI conference on artificial intelligence*, Vol. 31.
- [50] M Tan. 1995. rethinking model scaling for convolutional neural networks. *arXiv*. 2019 doi: 10.48550. *arXiv* (1905).

- [51] Liang Tong, Zhengzhang Chen, Jingchao Ni, Wei Cheng, Dongjin Song, Haifeng Chen, and Yevgeniy Vorobeychik. 2021. Facesec: A fine-grained robustness evaluation framework for face recognition systems. In *Proceedings of the IEEE/CVF Conference on Computer Vision and Pattern Recognition*. 13254–13263.
- [52] Laurens Van der Maaten and Geoffrey Hinton. 2008. Visualizing data using t-SNE. *Journal of machine learning research* 9, 11 (2008).
- [53] Zhou Wang, Alan C Bovik, Hamid R Sheikh, and Eero P Simoncelli. 2004. Image quality assessment: from error visibility to structural similarity. *IEEE transactions on image processing* 13, 4 (2004), 600–612.
- [54] Zhuo Wang, Zezheng Wang, Zitong Yu, Weihong Deng, Jiahong Li, Tingting Gao, and Zhongyuan Wang. 2022. Domain generalization via shuffled style assembly for face anti-spoofing. In *Proceedings of the IEEE/CVF Conference on Computer Vision and Pattern Recognition*. 4123–4133.
- [55] Zhenyu Wang, Xuemei Xie, Qinghang Zhao, and Guangming Shi. 2022. Filter clustering for compressing cnn model with better feature diversity. *IEEE Transactions on Circuits and Systems for Video Technology* (2022).
- [56] Matthew Watson and Noura Al Moubayed. 2021. Attack-agnostic adversarial detection on medical data using explainable machine learning. In *2020 25th International Conference on Pattern Recognition (ICPR)*. IEEE, 8180–8187.
- [57] Chen Wei, Karttikeya Mangalam, Po-Yao Huang, Yanghao Li, Haoqi Fan, Hu Xu, Huiyu Wang, Cihang Xie, Alan Yuille, and Christoph Feichtenhofer. 2023. Diffusion Models as Masked Autoencoders. *arXiv preprint arXiv:2304.03283* (2023).
- [58] Weihao Xia, Yulun Zhang, Yujiu Yang, Jing-Hao Xue, Bolei Zhou, and Ming-Hsuan Yang. 2022. Gan inversion: A survey. *IEEE Transactions on Pattern Analysis and Machine Intelligence* 45, 3 (2022), 3121–3138.
- [59] Weilai Xiang, Hongyu Yang, Di Huang, and Yunhong Wang. 2023. Denoising Diffusion Autoencoders are Unified Self-supervised Learners. *arXiv preprint arXiv:2303.09769* (2023).
- [60] Cihang Xie, Zhishuai Zhang, Yuyin Zhou, Song Bai, Jianyu Wang, Zhou Ren, and Alan L Yuille. 2019. Improving transferability of adversarial examples with input diversity. In *Proceedings of the IEEE/CVF conference on computer vision and pattern recognition*. 2730–2739.
- [61] Xiao Yang, Chang Liu, Longlong Xu, Yikai Wang, Yinpeng Dong, Ning Chen, Hang Su, and Jun Zhu. 2023. Towards Effective Adversarial Textured 3D Meshes on Physical Face Recognition. In *Proceedings of the IEEE/CVF Conference on Computer Vision and Pattern Recognition*. 4119–4128.
- [62] Zitong Yu, Rizhao Cai, Zhi Li, Wenhan Yang, Jingang Shi, and Alex C Kot. 2022. Benchmarking joint face spoofing and forgery detection with visual and physiological cues. *arXiv preprint arXiv:2208.05401* (2022).
- [63] Zitong Yu, Ajian Liu, Chenxu Zhao, Kevin HM Cheng, Xu Cheng, and Guoying Zhao. 2023. Flexible-modal face anti-spoofing: A benchmark. In *Proceedings of the IEEE/CVF Conference on Computer Vision and Pattern Recognition*. 6345–6350.
- [64] Zitong Yu, Chenxu Zhao, Zezheng Wang, Yunxiao Qin, Zhuo Su, Xiaobai Li, Feng Zhou, and Guoying Zhao. 2020. Searching central difference convolutional networks for face anti-spoofing. In *Proceedings of the IEEE/CVF Conference on Computer Vision and Pattern Recognition*. 5295–5305.
- [65] Kaipeng Zhang, Zhanpeng Zhang, Zhifeng Li, and Yu Qiao. 2016. Joint face detection and alignment using multitask cascaded convolutional networks. *IEEE signal processing letters* 23, 10 (2016), 1499–1503.
- [66] Richard Zhang, Phillip Isola, Alexei A Efros, Eli Shechtman, and Oliver Wang. 2018. The unreasonable effectiveness of deep features as a perceptual metric. In *Proceedings of the IEEE conference on computer vision and pattern recognition*. 586–595.
- [67] Wentian Zhang, Haozhe Liu, Feng Liu, Raghavendra Ramachandra, and Christoph Busch. 2022. Effective Presentation Attack Detection Driven by Face Related Task. In *European Conference on Computer Vision*. Springer, 408–423.

A ADVERSARIAL EXAMPLES

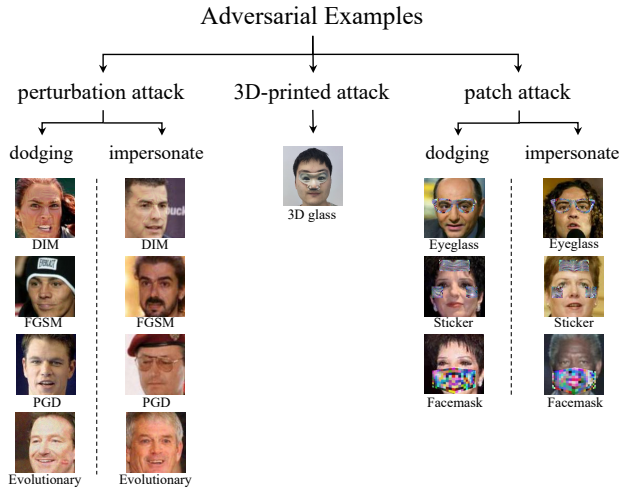


Figure 9: The adversarial examples with different attacks.

In this section, we present a comprehensive enumeration of all types of adversarial examples (as shown in Figure 9) along with the attack success rate for each type of attack (as illustrated in Table 8).

From the figure, it is evident that different adversarial examples exhibit distinct characteristics, particularly in terms of perturbations and patches, where the added information significantly varies. From the table, the generally close to 100% attack success rate indicates that adversarial attacks pose a significant threat to face recognition systems.

Table 8: The attack success rate of different attacks.

Attack	D/T	ASR(%)
FGSM(w)	Dodging	99.8
FGSM(w)	Impersonate	99.9
DIM(w)	Dodging	100.0
DIM(w)	Impersonate	100.0
PGD(w)	Dodging	100.0
PGD(w)	Impersonate	100.0
Evolutionary(b)	Dodging	99.6
Evolutionary(b)	Impersonate	98.7
Eyeglass(w)	Dodging	99.4
Eyeglass(w)	Impersonate	96.8
Sticker(w)	Dodging	99.1
Sticker(w)	Impersonate	97.4
Facemask(w)	Dodging	99.9
Facemask(w)	Impersonate	92.7